RESEARCH ARTICLE | JULY 28 2014

Role of the crystallization substrate on the photoluminescence properties of organo-lead mixed halides perovskites

Michele De Bastiani; Valerio D'Innocenzo; Samuel D. Stranks; Henry J. Snaith; Annamaria Petrozza

APL Mater. 2, 081509 (2014)
https://doi.org/10.1063/1.4889845

Role of the crystallization substrate on the photoluminescence properties of organo-lead mixed halides perovskites

Michele De Bastiani,[1,2,a] Valerio D'Innocenzo,[1,3,a] Samuel D. Stranks,[4] Henry J. Snaith,[4] and Annamaria Petrozza[1,b]
[1]*Center for Nano Science and Technology @Polimi, Istituto Italiano di Tecnologia, via Giovanni Pascoli 70/3, 20133 Milan, Italy*
[2]*Dipartimento di Scienze Chimiche, Università degli Studi di Padova, via Marzolo 1, 35131 Padova, Italy*
[3]*Dipartimento di Fisica, Politecnico di Milano, Piazza L. da Vinci, 32, 20133 Milano, Italy*
[4]*University of Oxford, Clarendon Laboratory, Parks Road, Oxford, OX1 3PU, United Kingdom*

(Received 8 May 2014; accepted 30 June 2014; published online 28 July 2014)

We have fabricated $CH_3NH_3PbI_{3-x}Cl_x$ perovskite thin films crystallized *in situ* on substrates of different natures (e.g., porosity, wettability) and investigated their photoluminescence properties. We observe that the crystallization time and thin film structure are strongly influenced by the chemical nature and porosity of the substrate. Moreover, we find that the mesoporous scaffold can tune the emissive properties of the semiconducting compound both in terms of spectral region and dynamics. In particular, perovskite crystallites grown in the nanometre size porous scaffold present a shorter-living and blue-shifted emission with respect to the perovskite crystals which are free to grow without any constraints. [http://dx.doi.org/10.1063/1.4889845]

In the last two years, perovskite based solar cells have been characterized by a fast development achieving impressive power conversion efficiencies up to 16.7%.[1–10] It has been demonstrated that organo-lead halide perovskite can work efficiently in a variety of device architectures going from a dye sensitized concept, in which the perovskite crystals replace the dye on the TiO_2 mesoporous scaffold,[7] to a meso-superstructured device architecture in which the TiO_2 is replaced by an Al_2O_3 mesoporous scaffold,[3] proving that the perovskite crystals can also sustain charge transport. As a further evolution, thin film architectures have been particularly successful[6,11,12] demonstrating performances comparable to traditional inorganic thin-film solar cells.[13,14] While we have borne witness to unbelievable progress and evolution of photovoltaic devices based on these materials, the huge gap in understanding when moving from the pristine molecules to their embodiment in a device can severely hamper their widespread adoption in optoelectronic applications. From the literature it is clear that every preliminary test of these materials in device architectures has revealed exciting surprises, however their working mechanisms remain remarkably obscure. Our poor understanding of the relationship between structure and optoelectronic properties is a key shortcoming, especially given that hybrid perovskites are intrinsically complex materials, where the presence of various types of interactions and structural disorder may play an important role in the material properties. The difficulty in predicting the response of these materials to the interaction with external stimuli makes it impossible to frame them as a proper technology. Due to the critical role of structural interactions of the organic/inorganic components, different crystallization/deposition methodologies

[a]M. De Bastiani and V. D'Innocenzo contributed equally to this work.
[b]Author to whom correspondence should be addressed. Electronic mail: annamaria.petrozza@iit.it

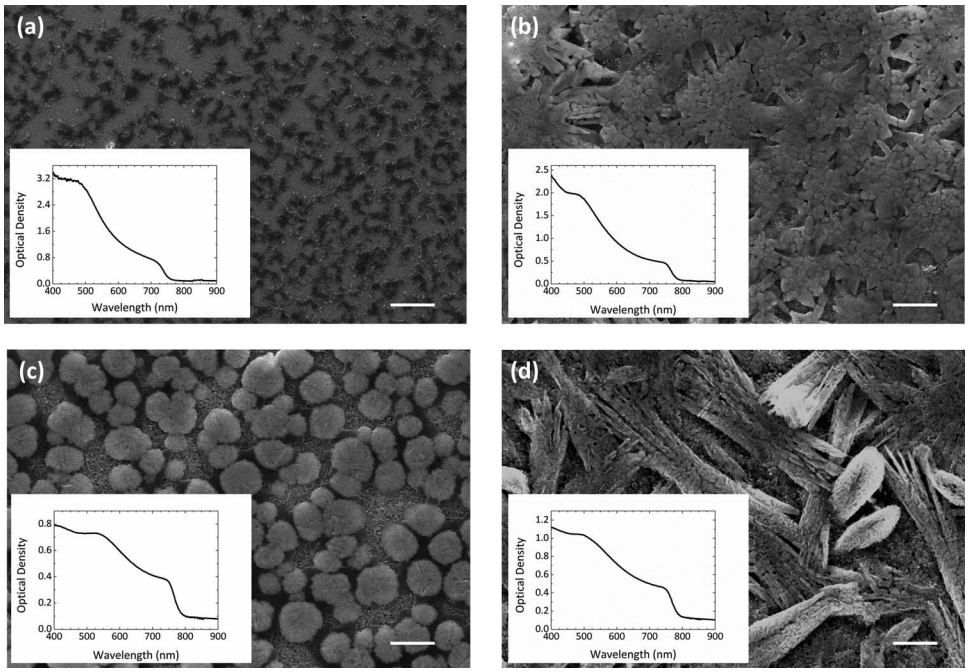

FIG. 1. SEM pictures (top view) of perovskite polycrystalline films grown on 1000 nm thick mesoporous Al_2O_3 scaffold (a) and ZnO scaffolds made of ZnO nanoparticles of 70 nm diameter (b), 50 nm diameter (c), and 20 nm diameter (d), respectively. Scale bar: 10 μm (a); 2 μm (b)–(d).

can lead to crystals with identical nominal chemical composition but with different macroscopic optoelectronic properties. In this work, we focus on the investigation of $CH_3NH_3PbI_{3-x}Cl_x$ perovskite thin films crystallized *in situ* on substrates of different natures (e.g., porosity, wettability) and on their photoluminescence properties.

ZnO nanoparticles (np) of three different sizes, 70 nm, 50 nm, and 20 nm, have been deposited by spin coating onto glass substrates in order to obtain about 1000 nm thick scaffolds with different porosities. Due to its low-temperature processability this oxide has a strong technological relevance,[15–17] in fact, it has already been employed as a selective contact in perovskite based solar cells both on rigid and flexible substrates showing good charge collection properties[18] and overall performances comparable to the most commonly used TiO_2.[9,19–21] At the same time a mesoporous scaffold of Al_2O_3 made of 50 nm nanoparticles, typically used in state of the art solar cells, was prepared. The metal-organic perovskite films were fabricated by spin coating on each substrate the precursor solution consisting of CH_3NH_3I and the $PbCl_2$ dissolved in a common solvent (see the supplementary material for details on sample fabrication[22]). For substrates such as TiO_2 and Al_2O_3, generally, after the deposition of the precursors the perovskite layer looks yellowish and transparent, meaning that the self-assembling of the crystal has not yet taken place. A heat treatment at 100 °C for 1 h is essential for initializing the nucleation of the crystallites, thus enabling the formation of the perovskites.[3,4,23,24] We found that after spin coating on different ZnO substrates the layer looks brownish by eye and after 1 min annealing at 100 °C the $CH_3NH_3PbI_{3-x}Cl_x$ is completely formed, as confirmed by absorption spectra[25] (see insets in Figure 1). Longer annealing time led to decomposition of the film. The reduction in the annealing time suggests a faster kinetic for the crystallization of the perovskites on ZnO substrates which can be mainly related to a different surface chemistry. Figure 1 shows the top view of the perovskite polycrystalline films. While the perovskite crystals of $CH_3NH_3PbI_{3-x}Cl_x$ are mainly formed in the Al_2O_3 scaffold with limited coverage of the capping layer left on top of the mesoporous substrate (Fig. 1(a)), the samples fabricated on the ZnO substrates show a consistent capping layer (Figs. 1(b)–1(d)). Interestingly, by changing the ZnO porosity it is possible to observe different crystalline macro-structures. In particular, we observe that nucleation on 70 nm ZnO np gives rise to interconnected structures (Figure 1(b)) of condensed domains in

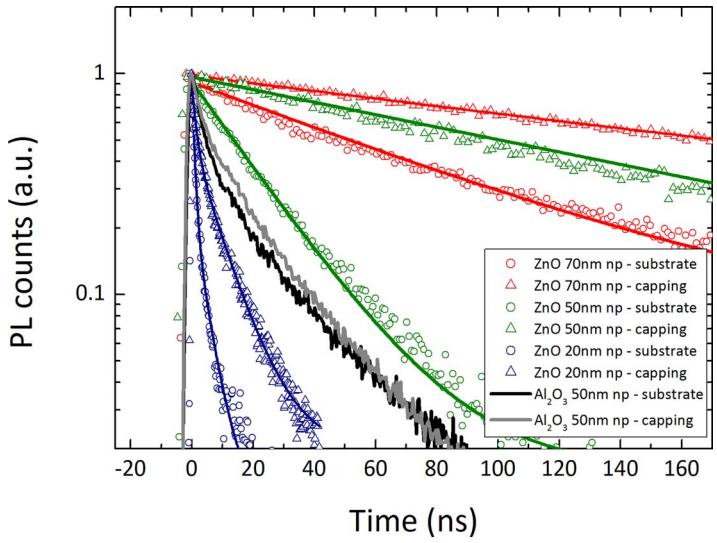

FIG. 2. Photoluminescence (PL) decays of $CH_3NH_3PbI_{3-x}Cl_x$ deposited on ZnO mesoporous scaffold substrates obtained from 20 nm (blue), 50 nm (green), and 70 nm (red) size ZnO nanoparticles, measured either exciting the sample from the substrate's side (circles) or from the capping layer side (triangles). Straight lines represent the fitting curves (Bi-exponential decay). The black and grey lines represent the PL decay of $CH_3NH_3PbI_{3-x}Cl_x$ deposited on mesoporous Al_2O_3 exciting the sample from substrate and capping layer sides, respectively. Excitation wavelength $\lambda_{exc} = 480$ nm, fluence of ~ 25 nJ/cm^2 (see the supplementary material for further information on experimental details[22]).

the range of a few microns of diameter. The structures obtained from 50 nm ZnO np are different from the previous one, in this case the capping layer is formed by islands with a circular shape (Figure 1(c)). However, the bridge-like interconnections between these structures are missing and the coverage of the capping layer in this scaffold is less with respect to the 70 nm scaffold, showing more mesoporous regions. A different morphology is also reported for $CH_3NH_3PbI_{3-x}Cl_x$ grown on 20 nm ZnO substrate (Figure 1(d)). Microns long fibril-like structures are obtained. These fibrils extend all over the substrate as a disoriented mat overlapping each other. Zooming inside the fibrils a crystalline structure partially oriented in the sense of the fibers with sub-micron domains can be observed, as shown in Figure S1 of the supplementary material.[22] These observations highlight a critical issue for the *in situ* crystallization, especially in a porous substrate, whose wettability will be affected not only by the chemical nature of the scaffold but also by its porosity. Directly after application of the precursor solution, the pores will be wet by the solution with an excess of solution on top. The ratio between infiltrated solution and excess solution on top will strongly depend on the wettability of the substrate. In agreement with what we observe, by measuring the Surface Free Energy (SFE) of the scaffolds under investigation[26,27] (see Table S1 of the supplementary material[22]), we find that the Al_2O_3 shows the highest SFE, while for the ZnO scaffold it will increase with increasing the nanoparticle size. In the initial stages of spin-coating a large quantity of solution flows off the substrate and as the spin-coating proceeds the solvent will evaporate from the surface of the wet film setting up a concentration gradient of the precursors within the film. The precursors will be driven via diffusion into the pores with the loss of solvent and increasing concentration. Of course, this process will critically affect the crystallization dynamics which can favor the stabilization of different phases in terms of crystals chemical composition, structure, and size.

We investigated how the substrate-induced morphological changes affect the photophysical properties of these compounds by time resolved photoluminescence (PL) spectroscopy. Figure 2 shows the PL decays taken from the samples shown in Figure 1, excited both from the capping layer side or the substrate side. The decays are taken at the peak of the photoluminescence band (see Figure S2 in the supplementary material[22]). A few interesting observations can be highlighted. Overall, the PL decays become shorter as the ZnO nanoparticles' size becomes smaller. Moreover, when comparing the decays upon excitation of the capping-layer side and the substrate side, one

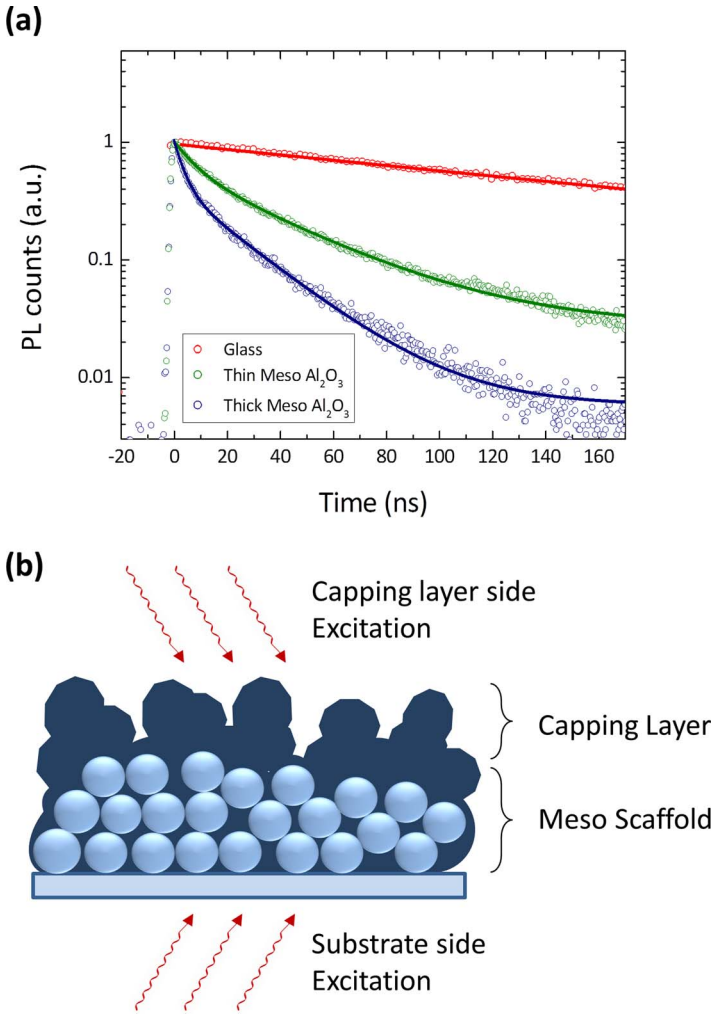

FIG. 3. (a) PL decay of $CH_3NH_3PbI_{3-x}Cl_x$ deposited on bare glass (red), thin (∼300 nm) mesoporous Al_2O_3 (green), and thick (∼800 nm) mesoporous Al_2O_3 (blue) together with the straight line representing the fitting curves (Bi-exponential decay). (b) Schematic representation of the layered structure of the samples investigated. Excitation wavelength $\lambda_{exc} = 480$ nm, fluence of ∼ 60 nJ/cm^2.

can also observe a further shortening in the lifetime in the latter case. Similar dynamics can also be observed in the presence of mesoporous TiO_2 substrates (see Figure S3 in the supplementary material[22]). As electron transfer from the perovskite to the ZnO is energetically favorable, at a first glance this can be attributed to a more efficient electron transfer in the presence of a larger density of interfaces due to the reduced average nanopores size. However, this conclusion does not appear really straightforward upon a deeper analysis. From the absorption spectra showed in the insets of Figure 1 we were able to estimate that the penetration depth of light at 480 nm ranges from ∼150 nm to ∼400 nm, thus exciting from the substrate side (scaffold thickness ∼1000 nm) ensures excitation of the perovskite nano-crystallites grown exclusively within the oxide scaffold (see pore filling in Figure S4 of the supplementary material[22]). Comparing the decay probed from perovskites grown in Al_2O_3 and ZnO scaffold, both made from 50 nm nanoparticles, one should expect a stronger PL quenching in the presence of the ZnO, as Al_2O_3 has a large band-gap which precludes charge transfer. However, for the 50 nm ZnO nanoparticle-based mesoporous substrate we do observe an even longer lifetime. In order to further investigate this issue the PL decays from perovskite polycrystalline films grown on a flat glass substrate, on a thin (∼300 nm) Al_2O_3 mesoporous scaffold (which will also present a large fraction of capping layer) and on a thick (∼800 nm) mesoporous scaffold (with a very small

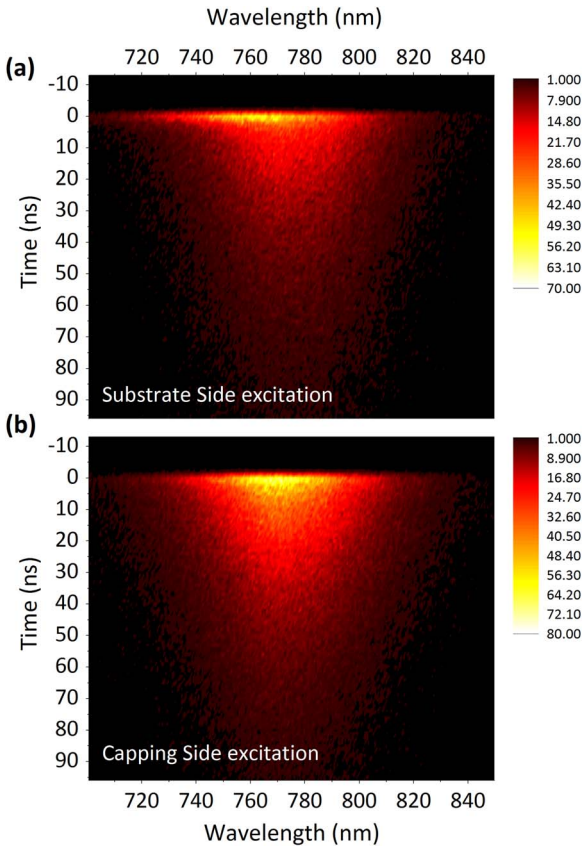

FIG. 4. PL maps of $CH_3NH_3PbI_{3-x}Cl_x$ deposited on thin mesoporous Al_2O_3 exciting the samples from the substrate side (a) and the capping layer side (b), respectively. Excitation wavelength $\lambda_{exc} = 480$ nm, fluence of ~ 60 nJ/cm^2.

fraction of capping layer) were measured and shown in Figure 3(a). The lifetime becomes shorter and shorter as the scaffold thickness is increased, i.e., increasing the contribution of crystallites grown in the scaffold to the overall PL signal with respect to the contribution coming from the crystals of the capping layer (schematic shown in Figure 3(b)). Figures 4(a) and 4(b) show 2D photoluminescence maps collected from the perovskite polycrystalline film grown on an even thinner Al_2O_3 scaffold ($\sim$100 nm) exciting from the substrate side and capping layer side, respectively. These maps show that when changing the side of excitation we can selectively observe two emissive states, one short living and blue shifted with respect to the other. In particular, we believe that the emission shown in Figure 4(a) arises from the superposition of two different contributions coming from the two layers in the thin film which get sequentially excited by the laser, i.e., the perovskite infiltrated into the mesoporous scaffold (short-living emission peaking around 760 nm) and the capping layer (long-living emission peaking at around 775 nm). This indicates that the shortening of the lifetime in presence of the scaffold is not simply due to PL quenching process, but it is related to an intrinsic change in the crystallite optoelectronic properties, in agreement with the absorption spectra taken from samples with similar architectures[28] showing that the fully mesostructured film is characterized by a blue-shifted absorption onset with respect to the flat film. Ball *et al.*[4] have already demonstrated that the perovskite crystals present in the capping layer are larger in size, going from less than 50 nm in the scaffold, where the crystal growth is constrained, to crystals larger than 500 nm when they are left to grow freely. Thus, we propose that the capping layer and the mesostructured film may be considered as two different compounds with different photoluminescence properties.

In summary, we demonstrate that the nature of the substrate critically affects the structural and optical properties of the perovskite films by changing the crystallization dynamics. We have observed that the $CH_3NH_3PbI_{3-x}Cl_x$ crystals form in only 1 min on ZnO substrates. This may have

drawbacks in terms of control of the final thin film structure. PL lifetime cannot be considered as an intrinsic property of the material due to the strong structure-property relationship in the self-assembled perovskites. Therefore, the PL lifetime quenching is not necessarily a good indicator for charge transfer at interfaces if the crystals structures are not entirely comparable at a molecular and mesoscopic level.

The authors thank Marina Gandini and Dr. Marcelo Alcocer for help with the experimental set-ups, Luca Passoni for help with the SEM set up, and Dr. Giulia Grancini for useful discussions. The research leading to these results has received funding from the European Union Seventh Framework Programme [FP7/2007–2013] under Grant Agreement No. 604032 of the MESO project.

[1] H. J. Snaith, J. Phys. Chem. Lett. **4**, 3623 (2013).
[2] H.-S. Kim, S. H. Im, and N.-G. Park, J. Phys. Chem. C **118**, 5615 (2014).
[3] M. M. Lee, J. Teuscher, T. Miyasaka, T. N. Murakami, and H. J. Snaith, Science **338**, 643 (2012).
[4] J. M. Ball, M. M. Lee, A. Hey, and H. J. Snaith, Energy Environ. Sci. **6**, 1739 (2013).
[5] J. You, Z. Hong, Y. M. Yang, Q. Chen, M. Cai, T. Song, C. Chen, S. Lu, Y. Liu, H. Zhou, and Y. Yang, ACS Nano **8**, 1674 (2014).
[6] M. Liu, M. B. Johnston, and H. J. Snaith, Nature **501**, 395 (2013).
[7] H.-S. Kim, C.-R. Lee, J.-H. Im, K.-B. Lee, T. Moehl, A. Marchioro, S.-J. Moon, R. Humphry-Baker, J.-H. Yum, J. E. Moser, M. Grätzel, and N.-G. Park, Sci. Rep. **2**, 591 (2012).
[8] T. C. Sum and N. Mathews, Energy Environ. Sci. **7**, 2518 (2014).
[9] D. Liu and T. L. Kelly, Nat. Photonics **8**, 133 (2013).
[10] N. J. Jeon, H. G. Lee, Y. C. Kim, J. Seo, J. H. Noh, J. Lee, and S. Il Seok, J. Am. Chem. Soc. **136**, 7837–7840 (2014).
[11] B. Conings, L. Baeten, C. De Dobbelaere, J. D'Haen, J. Manca, and H.-G. Boyen, Adv. Mater. **26**, 2041 (2014).
[12] Q. Chen, H. Zhou, Z. Hong, S. Luo, H.-S. Duan, H.-H. Wang, Y. Liu, G. Li, and Y. Yang, J. Am. Chem. Soc. **136**, 622 (2014).
[13] N. Asim, K. Sopian, S. Ahmadi, K. Saeedfar, M. A. Alghoul, O. Saadatian, and S. H. Zaidi, Renewable Sustainable Energy Rev. **16**, 5834 (2012).
[14] W. A. Badawy, "A review on solar cells from Si-single crystals to porous materials and quantum dots," J. Adv. Res. (to be published).
[15] Y. Sun, J. H. Seo, C. J. Takacs, J. Seifter, and A. J. Heeger, Adv. Mater. **23**, 1679 (2011).
[16] J.-S. Huang and C.-F. Lin, J. Appl. Phys. **103**, 014304 (2008).
[17] L. Li, T. Zhai, Y. Bando, and D. Golberg, Nano Energy **1**, 91 (2012).
[18] D. Son, J. Im, H. Kim, and N. Park, "11% Efficient Perovskite Solar Cell Based on ZnO Nanorods: An Effective Charge Collection System," J. Phys. Chem. (to be published).
[19] D. Bi, L. Yang, G. Boschloo, A. Hagfeldt, and E. M. J. Johansson, J. Phys. Chem. Lett. **4**, 1532 (2013).
[20] M. H. Kumar, N. Yantara, S. Dharani, M. Graetzel, S. Mhaisalkar, P. P. Boix, and N. Mathews, Chem. Commun. (Cambridge) **49**, 11089 (2013).
[21] E. J. Juarez-Perez, M. Wußler, F. Fabregat-Santiago, K. Lakus-Wollny, E. Mankel, T. Mayer, W. Jaegermann, and I. Mora-Sero, J. Phys. Chem. Lett. **5**, 680 (2014).
[22] See supplementary material at http://dx.doi.org/10.1063/1.4889845 for top view and cross sectional SEM of perovskite deposited on ZnO scaffold, the SFE table and spectral emission graphs of both ZnO and Al_2O_3 samples, and for details on experimental methods.
[23] G. E. Eperon, V. M. Burlakov, P. Docampo, A. Goriely, and H. J. Snaith, Adv. Funct. Mater. **24**, 151 (2014).
[24] Y. Zhao and K. Zhu, J. Phys. Chem. C **118**, 9412 (2014).
[25] A. Dualeh, N. Tétreault, T. Moehl, P. Gao, M. K. Nazeeruddin, and M. Grätzel, Adv. Funct. Mater. **24**, 3250 (2014).
[26] G. Cappelletti, S. Ardizzone, D. Meroni, G. Soliveri, M. Ceotto, C. Biaggi, M. Benaglia, and L. Raimondi, J. Colloid Interface Sci. **389**, 284 (2013).
[27] D. H. Kaelble, J. Adhes. **2**, 66 (1970).
[28] V. D'Innocenzo, G. Grancini, M. J. P. Alcocer, A. R. S. Kandada, S. D. Stranks, M. M. Lee, G. Lanzani, H. J. Snaith, and A. Petrozza, Nat. Commun. **5**, 1 (2014).